

Kinetics of radiative recombinations in GaSe and influence of Cu doping on the luminescence spectra

Vito Capozzi

*Dipartimento di Fisica, Università Delgi Studi di Trento, I-38050 Povo, Trento, Italy
and Gruppo Nazionale di Struttura della Materia del Consiglio Nazionale delle Ricerche, Trento, Italy*

(Received 23 November 1982)

Spontaneous photoluminescence (PL) spectra of Cu-doped and undoped ϵ -GaSe have been investigated in the temperature range from 80 to 300 K and at low laser-excitation intensity (P) from 10^{-3} to 10 W cm $^{-2}$. The main modification of the spectra in doped crystals with respect to those of undoped samples is the appearance of two bands in the extrinsic part of the PL spectrum and centered at 655 and 678 nm, respectively. The luminescence at energies below the excitonic recombinations (extrinsic bands) is enhanced by doping. Also indirect free- and bound-excitonic lines are also strongly influenced by the impurity concentration; in fact, their emission intensity, which depends linearly on P in undoped crystals, shows a quadratic dependence in doped samples. The temperature dependence of the PL spectra gives the thermal activation energy of some extrinsic bands, which results equal the ionization energy of the acceptor levels involved in the extrinsic transitions. A simple kinetic model of the radiative recombination is proposed; it accounts for the experimental data of the excitation intensity dependence of the free- and bound-excitonic lines. This model can also explain the different temperature dependence of the PL intensity of these lines: linear for the free-excitonic emissions, exponential for the bound-excitonic recombinations. Some radiative transitions from donor levels located in the energy gap of GaSe are analyzed and a scheme of donor and acceptor states involved in the PL spectra is proposed.

I. INTRODUCTION

The covalently bounded layers of the III-VI semiconductor compound GaSe contain four monatomic sheets in the order Se-Ga-Ga-Se. The single layer is hexagonal and the c axis is perpendicular to the layer plane. Several polytypes have been reported in the literature, which differ in the sequence of the basic layer units. The stacking sequences which occur most often are of the hexagonal ϵ ($2H$) and of the rhombohedral γ ($3R$) type,¹ belonging to the space groups D_{3h}^1 ($P\bar{6}m2$) and C_{3v}^5 ($R3m$), respectively. The mechanical properties of GaSe are strongly anisotropic; the electronic ones are less^{2,3} because of the considerable charge density located between the layers.⁴

The electronic band structure of gallium selenide, calculated using the empirical pseudopotential method⁵⁻⁷ shows the existence of a low-lying indirect gap in GaSe. In particular these authors predicted the presence of an indirect minimum of the conduction band (CB) at the M point of the Brillouin zone, lower than the direct one at the Γ point and they located the top of the valence band (VB) at the center of the Brillouin zone. These calculations essentially agree with those obtained recently by Nagel *et al.*⁴ using the tight-binding method.

In recent years, different experimental findings seem to confirm this model as illustrated by Le Chi Thanh and Depeursinge⁸ and by Abullaev *et al.*⁹ on the basis of absorption measurements. These results are compatible with the direct resonant-exciton model invoked by Mercier *et al.*¹⁰

Optical transitions between the top of the VB and the direct minimum (at Γ) of the CB are full allowed, if the electric field of the light is parallel to the c axis; for $\vec{E} \perp c$ the transition is weakly allowed, due to spin-orbit coupling, and its probability is about 2 orders of magnitude weaker than that for $\vec{E} \parallel c$.¹¹ The same selection rules are valid for the creation and recombination of direct and indirect excitons.^{5,11}

The excitonic features of GaSe have been extensively studied by several authors.¹¹⁻¹⁶ Comparatively little information is available on the energy levels in the forbidden energy gap.¹⁷ As far as these properties are concerned, this paper reports the comparison of spontaneous photoluminescence (PL) spectra of "undoped" (not intentionally doped) and Cu-doped GaSe single crystals, in the wavelength interval including the excitonic and extrinsic emission and in the temperature range from 80 to 300 K.

The choice of copper as the doping element was made because it noticeably influences the characteristics of the material, as indicated by the strong decrease of the electrical resistivity.¹⁸ In fact, a p -type conductivity from 10^{-3} to 10^{-4} Ω^{-1} cm $^{-1}$ was found in Cu-doped crystals, i.e., a value about 10^3 times higher than the corresponding value of undoped GaSe grown from the melting.

As regards the emission spectra of Cu-doped samples, two new bands centered at 655 and 678 nm appear below the excitonic structure (at 80 K). The PL spectra are analyzed as functions of exciting intensity and temperature; a model for the recombination kinetics is developed, which accounts for the experimental data reported below.

II. EXPERIMENTAL METHODS

The single crystals of GaSe were grown from the melt by the Bridgman technique.¹⁹ As reported in Ref. 20, we found by x-ray analysis and by excitonic transmission spectra that most of our samples were of ϵ type and very few (some percent) of γ type. All the samples investigated for this work had the ϵ -polytype structure. Undoped crystals showed an electrical conductivity of p type with $N_A - N_D \approx 10^{12} \text{ cm}^{-3}$ and $N_A + N_D \approx 10^{17} \text{ cm}^{-3}$, where N_A and N_D are the concentrations of donors and acceptors, respectively.¹⁸ Some crystals were intentionally doped by the addition of about 10^{20} cm^{-3} of copper atoms into the growth ampoules. A concentration of about $5 \times 10^{18} \text{ cm}^{-3}$ of Cu was detected by electrical transport measurements.¹⁹

The crystals were cleaved along the layers, obtaining platelets of about 1 cm^{-2} of area and 0.1 to 0.5 mm of thickness. The surface of the samples were irradiated along the c axis by a cw argon-ion laser using the 5145-Å line. The samples were attached to the copper cold finger of a liquid-nitrogen cryostat, the temperature of which could vary from 80 to 300 K by means of a thermoregulator having an accuracy of 1 K. The emission was collected in the backscattering geometry from the face of the crystal and analyzed by a double monochromator. The luminescence was detected by a cooled RCA C31034 photomultiplier and recorded by the standard lock-in technique. A set of neutral-density filters changed the intensity of the laser beam in the range from $10^{-3} \text{ W cm}^{-2}$ to 10 W cm^{-2} .

III. EXPERIMENTAL RESULTS

Figure 1 shows three photoluminescence spectra of Cu-doped GaSe, measured at the temperature of 80 K and for three excitation intensities (P). Other three luminescence spectra of an undoped GaSe crystal at the same temperature $T = 80 \text{ K}$ and for three values of P are reported in Fig. 2.

An evident feature in the PL spectra of the doped samples is the presence of the two bands R_1 and R_2 (centered at 655 and 678 nm, respectively [see Figs. 1(b) and 1(c)]), which have never been detected in all the undoped samples investigated. Apart from these two bands, the other lines of the spectra [(b) and (c) of Fig. 1] are also visible in the spectra (b) and (c) of Fig. 2. The spectra of these two figures can be divided in two parts: the first one includes the lines A , B , C , and D (intrinsic lines), while the second one comprises the remaining part of the luminescence lines, from E to H (extrinsic lines).

An important feature of the two kinds of crystals is the behavior of the PL spectra as a function of the excitation intensity. In fact, the extrinsic lines, which at the lowest values of P used in this experiment are more intense than the intrinsic lines [see Figs. 1(c) and 2(c)], become lower and lower and tend to saturate with respect to the intrinsic lines, when P increases [compare Fig. 1 with Fig. 2 going from the spectrum (c) and (a)]. Moreover, at higher excitation intensities (magnitude order of 10^2 mW cm^{-2}) the extrinsic lines of doped samples merge into a featureless band centered at 650 nm [see Fig. 1(a)].

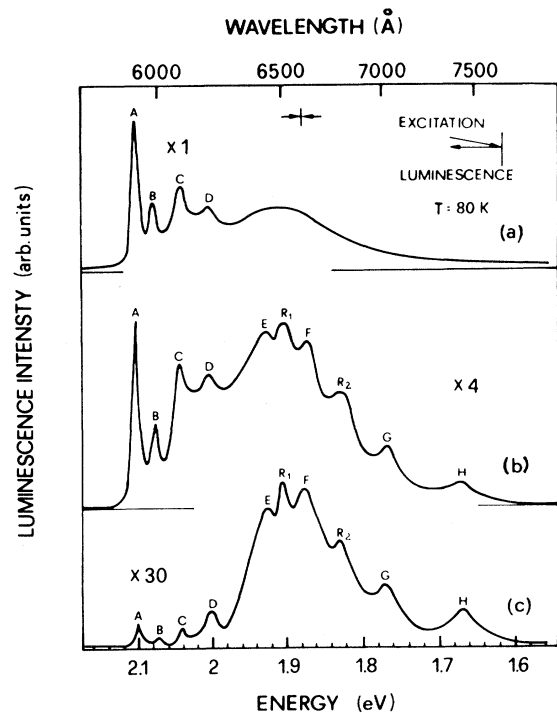


FIG. 1. Photoluminescence spectra of Cu-doped GaSe at 80 K. Light is collected from the face perpendicular to the c axis at three different excitation intensities: (a) 700 mW/cm^2 , (b) 40 mW/cm^2 , and (c) 3 mW/cm^2 . The denomination of lines is the same of Table I.

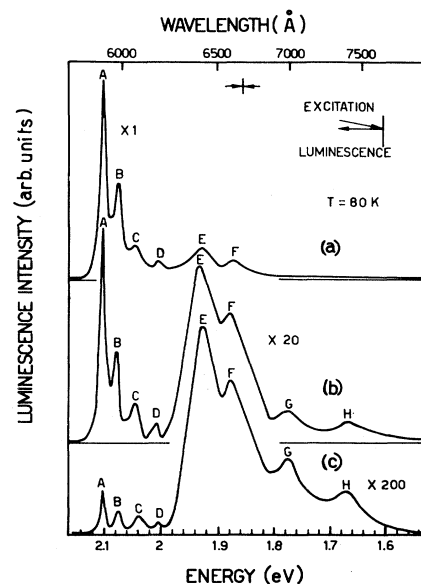


FIG. 2. Same as Fig. 1 for an undoped sample. The excitation intensities are (a) 400 mW/cm^2 , (b) 40 mW/cm^2 , and (c) 3 mW/cm^2 .

TABLE I. Results of photoluminescence spectra in undoped and Cu-doped GaSe at 80 K.

	Denomination of lines and wavelength (Å)	Energy (eV)	Power exponent γ Eq. (1)	ΔE (meV)		Luminescence intensity relative to A (80 K and 40 mW/cm ²)
				Eq. (1)	Eq. (2)	
GaSe undoped	<i>A</i>	5910±1	2.098	1.3		1.0
	<i>B</i>	5976±1	2.075	1.3	23±1	0.5
	<i>C</i>	6092±1	2.035	1.0		0.3
	<i>D</i>	6203±1	1.999	1.0	52±2	0.15
	<i>E</i>	6448±1	1.923	0.5		3.0
	<i>F</i>	6622±1	1.872	0.5	51±2	1.5
	<i>G</i>	7003±1	1.771	0.5	150±3	0.3
	<i>H</i>	7418±1	1.672	0.5		0.2
GaSe Cu-doped	<i>A</i>	5910±1	2.098	1.3		1.0
	<i>B</i>	5976±1	2.075	1.3	23±1	0.5
	<i>C</i>	6092±1	2.035	2.0		1.8
	<i>D</i>	6203±1	1.999	2.0	52±2	1.3
	<i>E</i>	6447±1	1.923	1.0		3.5
	<i>R</i> ₁	6552±1	1.892	1.0	30±1	4.0
	<i>F</i>	6622±1	1.872	1.0	51±2	3.5
	<i>R</i> ₂	6775±1	1.830	1.0	91±3	1.8
	<i>G</i>	7001±1	1.771	0.5	153±5	0.8
	<i>H</i>	7417±1	1.672	0.5		0.5

The bands *E*, *F*, *G*, and *H* are present in both types of samples, but their intensity, relative to that of the direct free exciton, is higher in doped samples; this fact indicates that the Cu doping is not directly responsible for all localized extrinsic levels, but it influences their density. It has been suggested²¹ that the Cu atoms intercalate between the layers of GaSe; in the crystals, this can increase the number of stacking faults which are due to the weak interlayer interactions.²⁰ This enhancing of extrinsic levels with doping is also consistent with the fact that saturation effects of extrinsic bands are barely visible in doped samples, while they are easily seen at the highest excitations in undoped ones [see Fig. 3 and Fig. 2(a), where the lines *G* and *H* are already saturated].

The relative intensities of the lines varied sometimes from sample to sample, but the energy positions remained constant in all investigated crystals. The spectra have been analyzed by decomposing them into a series of overlapping Gaussians, using as fitting parameters amplitude, halfwidth, and center energy. This procedure has been applied only to spectra in which the structures are reasonably well defined. Other line shapes have been tried: The results are approximately the same (considering the errors) as those obtained from Gaussian bands. At the same time, the overlapping of band tails does not permit one to discriminate between the various line shapes. The Gaussian lines have been used only as a means for analyzing the PL spectra quantitatively. The results of these deconvolutions are reported in Table I.

Figures 3(a) and 3(b) show the dependences of the intensity of some intrinsic and extrinsic lines versus excitation intensity for (a) undoped and (b) doped samples. In Fig. 3(b), lines *A* and *B* have been omitted for clarity, because their behavior is exactly the same as that of their corresponding lines in undoped samples (see Table I).

The experimental data of various bands of Fig. 3 can be

fitted, excluding the saturation region at the highest intensities, by the simple power law,

$$L \propto P^\gamma, \quad (1)$$

where L is the integrated luminescence intensity of the bands, P is the excitation laser intensity, and γ is an adimensional exponent.

The most prominent features of Figs. 3(a) and 3(b) are (a) lines *C* and *D*, which depend linearly ($\gamma = 1$) on P in undoped crystals, show a quadratic dependence ($\gamma = 2$) in Cu-doped samples. (b) The remaining extrinsic lines are characterized by linear or sublinear dependences. In particular, the intensity of *E* and *F*, which shows a square-root dependence followed by a saturation in undoped crystals, depends linearly on P in doped ones (see Table I). The lines *G* and *H* behave similarly in undoped and doped

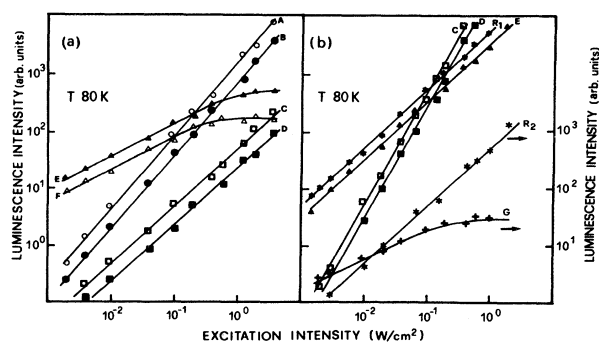


FIG. 3. Luminescence intensity of various lines vs excitation intensities at 80 K: for (a) undoped crystals and (b) Cu-doped crystals.

crystals: i.e., their intensity increases first sublinearly ($y = 0.5$) with P , and then saturates, as shown in Fig. 3(b) for the line G . In the figures 3(a) and 3(b) all the extrinsic lines are not reported, but their main features and results are summarized in Table I.

The luminescence intensity of the excitonic lines and some extrinsic bands, as a function of T , is reported in Fig. 4, at constant photoexcitation intensity. The temperature dependence of the intensity of the lines A , B , C , and D is the same for both doped and undoped samples, i.e., linear for A and C , exponential for B and D , as shown in Fig. 4(a) and Fig. 4(b), respectively.

The intensity of E in both types of samples is nearly constant up to about 180–200 K, while at higher temperature it decreases abruptly [see Fig. 4(c)]. For the other extrinsic lines, the experiment data can be fitted by the following equation [continuous lines in Fig. 4(c)]:

$$L \propto \exp(\Delta E/kT), \quad (2)$$

where ΔE is the thermal activation energy and k the Boltzmann constant. The values of ΔE obtained for doped and undoped samples are reported in Table I.

Moreover, it is useful to remark here (see discussion below) that the energy differences between the parts (A, B) and (C, D), are equal to the value of ΔE deduced from Eq. (2) for the lines B and D , respectively. Table I summarizes the results which are deduced from the analysis of Figs. 1 to 4. At temperatures higher than 200 K only the lines A and B are still visible in the PL spectra of both types of crystals.

IV. DISCUSSION

A. Intrinsic lines

The line A at 2.098 eV is attributed to the well-known recombination of the direct free exciton (DFE) associated to the direct conduction band.¹² The ionization energy of the DFE is about 20 meV (Ref. 17) and then the bottom of the direct CB at 80 K lies at about 2.118 eV above the top of VB.

In agreement with the absorption measurements reported by Abdullaev *et al.*,⁹ the line C at 2.035 eV can be ascribed to the radiative decay of the indirect free excitons (IFE), associated to the indirect conduction band (ICB). This indirect transition occurs with the emission of an A_1' phonon of 15 meV. The assignment of the line C agrees also with the luminescence results of Mercier *et al.*¹⁰ who found (at 77 K) the minimum M of the indirect gap located at 2.093 eV above the top of VB. From the energy position of the line C and that of the above phonon, an estimation of about 2.050 eV results for IFE.

The luminescence intensity of the line B increases with P , in the same way as the line A [see Fig. 3(a)]. Moreover, the exponential thermal quenching of this line, reported in Fig. 4(b), gives an activation energy ΔE which is the same as the energy difference between the lines A and B (see Table I). These results suggest that B can be due to the recombination of direct bound exciton (DBE) to impurity centers localized in the energy gap of crystals. As proposed in Ref. 22, these binding impurities could be the

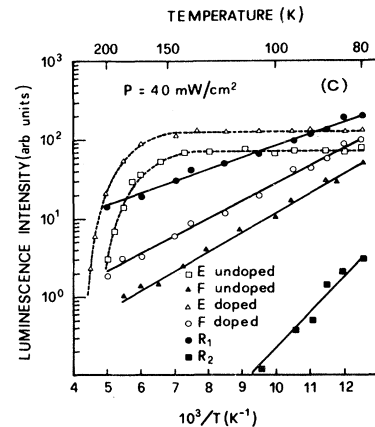
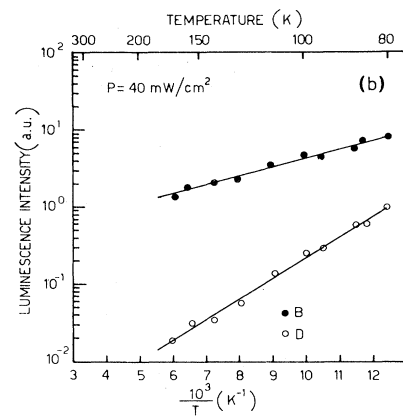
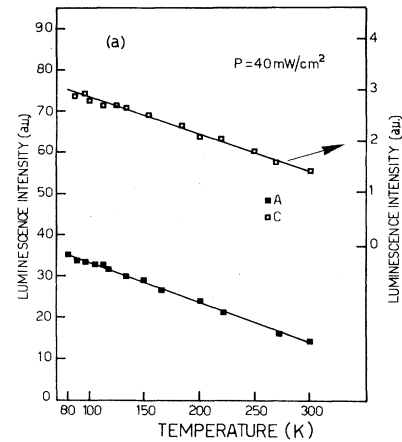


FIG. 4. (a) Temperature dependence of the excitonic lines A and C at the photoexcitation intensity of 40 mW/cm^2 , (b) semi-log plot of the intensity of the lines B and D vs $(1/T)$ at 40 mW/cm^2 , and (c) temperature dependence of the emission intensity of some extrinsic lines at 40 mW/cm^2 . In (b) and (c) the continuous straight lines are the least-squares fits of experimental points to Eq. (2) of the text.

donor levels d_1 at about 0.195 eV below DCB and detected by electrical transport measurements.¹⁸

Similar results are obtained for the line D , i.e., the intensity of D increases linearly with P , as the line C does [Fig. 3(a)] and decreases exponentially when T increases [Fig. 4(b)]. Moreover, the activation energy ΔE deduced from Eq. (2) is also equal to the energy difference between IFE and the line D . These results and the assignment of the line C , as the indirect free-exciton recombination, suggest that the line D in agreement with Ref. 22, can also be attributed to the recombination of indirect bound excitons (IBE) to localized centers in the energy gap. These centers could be the deep level d_2 at 0.42 eV below ICB, as discussed previously.²²

The presence of donorlike levels in p -type samples is consistent with the high compensation observed by electrical measurements.¹⁹ The quenching of the lines B and D as T increases can be attributed to the thermal freeing of direct and indirect excitons, respectively, from their binding centers.

B. Recombination kinetics

In GaSe two main radiative recombination channels are possible: (i) recombination at the direct and indirect gap via free- and bound-excitonic states, and (ii) recombination via impurity levels localized in the forbidden gap.

The importance of the direct recombination channel in gallium selenide is due to the fact that the direct exciton is resonant with the continuum states of the indirect minimum M .¹⁰ In any case, the presence of impurity states, low pumping power, and low temperature tend to favor indirect recombinations. This fact is evident from a comparison of Figs. 1 and 2, in which C and D lines are more pronounced in doped materials. The same conclusions can be drawn as far as temperature and pumping power are concerned.¹⁷

The indirect channel is strongly influenced by impurity levels as reported in Table I, which shows the change of the exponent for the pumping dependence—Eq. (1)—of integrated emission intensity of C and D lines. This change can be justified by the kinetic model outlined in Fig. 5. In developing the model we assume that in the steady state electrons and holes, as well as excitons, obey a Boltzmann distribution with a temperature T near to that of the crystals. Then it is reasonable to assume that the fraction of the optically excited carriers, which thermalize at the indirect band minimum, is proportional to the excitation intensity. This hypothesis decouples the direct and indirect channels and permits to consider them separately.

We describe the kinetics of indirect recombinations by using three rate equations for the population of levels IFE, IBE, and IL (see Fig. 5). The levels below IBE are lumped together in the impurity states IL. The photoelectrons thermalizing at ICB immediately bind to holes, thereby forming excitons, or alternatively, they are trapped at impurity levels. Within this assumption, the ICB states are considered only as an intermediate step, occurring very rapidly. This hypothesis agrees with the fact that indirect band recombinations have not yet been observed. Consequently, in the rate equations for the states IFE and IL the

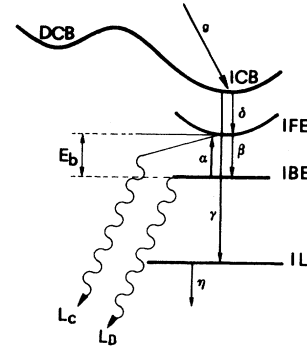


FIG. 5. Simplified recombination model for the lines C and D : ICB is the indirect conduction-band minimum, IFE is the indirect free-exciton level, IBE is the indirect bound-exciton level, and IL are the impurity levels. E_b is the exciton-to-impurity binding energy and L_C , L_D are emitted intensities of IFE and IBE, respectively. g is the generation rate and α , β , γ , δ , and η are transition-rate coefficients.

generation terms are written δg and $\gamma g(N_i - n_i)$, respectively (see the list of symbols below).

The factor $(N_i - n_i)$ takes into account the limited number of impurity states, as compared with free-exciton states, for which the generation rate is taken proportional to g alone. Moreover, the fact that all photoexcited electrons contribute very rapidly either to the free-exciton population or to the fraction of the electrons trapped at impurities, permits one to write the following condition

$$g = \delta g + \gamma g(N_i - n_i). \quad (3)$$

Then the resulting rate equations are

$$\begin{aligned} \frac{dn_{fe}}{dt} &= \frac{-n_{fe}}{\tau_{fe}} + \delta g + \alpha n_{be} \exp\left[-\frac{E_b}{kT}\right] \\ &\quad - \beta n_{fe}(N - n_{be}) = 0, \end{aligned} \quad (4a)$$

$$\begin{aligned} \frac{dn_{be}}{dt} &= \frac{-n_{be}}{\tau_{be}} - \alpha n_{be} \exp\left[-\frac{E_b}{kT}\right] \\ &\quad + \beta(N - n_{be})n_{fe} = 0, \end{aligned} \quad (4b)$$

$$\frac{dn_i}{dt} = \gamma g(N_i - n_i) - \eta n_i = 0. \quad (4c)$$

The meaning of the symbols used in the above three equations is the following: n_{fe} (n_{be}), free- (bound-) indirect-exciton level population; τ_{fe} (τ_{be}), free- (bound-) indirect-exciton life time; α , β , γ , δ , and η , transition rate coefficients; E_b , indirect exciton to impurity binding energy; g , fraction of nonequilibrium carriers thermalizing into the indirect gap; N , total density of d_2 impurity levels to which indirect excitons bind; N_i , total density of IL levels; and n_i , density of IL levels filled with electrons.

By solving Eq. (4), using the condition (3) and assuming, reasonably, $n_{be} \ll N$ one obtains

$$L_D = \frac{n_{be}}{\tau_{be}} = g \frac{\eta(1 - \gamma N_i) + \gamma g}{\eta + \gamma g} \times \left[1 + \frac{\alpha \tau_{be} \exp(-E_b/kT)}{\tau_{fe} \beta N} \right]^{-1}, \quad (5)$$

where L_D is the luminescence intensity of the D line (indirect bound-exciton decay).

From Eq. (5), it can be easily seen that the following limiting dependences are possible when T is constant:

$$\begin{aligned} L_D &\propto g \quad \text{when } g \ll \eta \left[\frac{1}{\gamma} - N_i \right] < \frac{\eta}{\gamma}, \\ L_D &\propto g^2 \quad \text{when } \eta \left[\frac{1}{\gamma} - N_i \right] \ll g \ll \frac{\eta}{\gamma}, \\ L_D &\propto g \quad \text{when } \eta \left[\frac{1}{\gamma} - N_i \right] < \frac{\eta}{\gamma} \ll g. \end{aligned} \quad (6)$$

The interval of g in which the square dependence is possible is dependent on N_i and becomes practically zero for $N_i \ll 1/\gamma$, i.e., low-impurity concentrations, in agreement with the experimental data of the D line reported in Figs. 3(a) and 3(b) and Table I.

At present, measurements are in progress on GaSe samples doped with different impurity concentrations. The preliminary results obtained²³ confirm the above considerations summarized in Eq. (6).

The same conclusion can be drawn for the indirect free-exciton emission L_C which is given by

$$L_C = \frac{n_{fe}}{\tau_{fe}} = L_D \frac{1 + \alpha \exp(-E_b/kT) \tau_{be}}{\beta N \tau_{fe}} \propto L_D. \quad (7)$$

Moreover, Eqs. (5) and (7) could justify also the different temperature dependences of C and D lines reported in Figs. 4(a) and 4(b), respectively, i.e., linear for the line C , exponential for the line D . In fact, assuming

$$\tau_{be} \alpha \exp(-E_b/kT) \gg 1, \quad (8a)$$

$$\tau_{be} \alpha \exp(-E_b/kT) \gg \tau_{fe} \beta N, \quad (8b)$$

one obtains

$$L_D \propto \exp(E_b/kT), \quad (9)$$

$$L_C \simeq \text{const}. \quad (10)$$

In the same way, analogous results are obtained for the direct recombinations of the free (line A) and bound (line B) excitonic emission. The weak linear dependence on T of L_C and L_A can be explained by the variation of parameters such as lifetimes and rate coefficients, which in the above analysis have been assumed to be constant.

It is difficult to assess the validity of the approximation used above to explain the temperature dependence of C and D lines. In fact, no information is currently available concerning the lifetime of indirect excitons and their transition rate at impurities in GaSe. Consequently the above approximations are to be mainly considered necessary conditions required by experimental data.

The condition (8a) implies that the bound-exciton dissociation rate is much greater than the bound-exciton recombination rate, which is reasonable at $T \geq 80$ K. Moreover, taking into account the very short lifetime (about 10^{-10} s) of the direct free exciton,²⁴ this order of magnitude is probably true also for the indirect one. Consequently, the recombination rate of the indirect free exciton is approximately greater than its rate of binding. This means

$$\frac{n_{fe}}{\tau_{fe}} \geq \beta N n_{fe} \quad (\text{with } N \gg n_{be}),$$

i.e., $\beta N \tau_{fe} \lesssim 1$, which together with the condition (8a) gives the inequality (8b).

C. Analysis of the extrinsic luminescence bands

The lines E , F , G , H , R_1 , and R_2 are due to radiative recombination of trapped photoelectrons via intragap defect states. R_1 and R_2 are connected to the Cu doping, and they can be ascribed to bound-bound transitions between the donor level d_1 , which is also responsible for the bound-exciton B line and acceptor levels located at 31 and 93 meV above VB. The first of these levels is practically coincident with the acceptor level found for Cu-doped samples.¹⁹ Moreover, the intensity of R_1 and R_2 have an exponential thermal quenching with $\Delta E = 30$ and 91 meV, respectively. This is an indication that the thermal activation energy of the luminescence intensity of these two bands is equal to the ionization energy of a_2 and a_4 acceptor levels reported in Fig. 6.

The radiative recombination of an electron (trapped at a donor) with a hole (trapped at an acceptor) will result at an energy which will depend on the separating distance between the donor and acceptor.²⁵ Moreover, it is evident that this separation depends on the excitation intensity of the crystal. Effectively, we have observed that increasing the pumping excitation, the peaks of R_1 and R_2 move to higher energy and at the same time the two bands become larger. However, this shift was only a few angstroms because of the small range of excitation intensity of this work. In fact, in other semiconductors (GaP for example) a variation of several orders of magnitude were needed to get a shift of a few meV.²⁶

Concerning the lines E , F , G , and H , they are present also in undoped crystals, although they are enhanced by the doping. They can be explained (see Fig. 6) by assuming transitions from the same levels d_1 and d_2 to the valence band (E and H) and to localized states at 51 and 152 meV above the VB (F and G). Levels at about the same energy have been detected by other authors (see Table II and Ref. 27) by means of electrical transport measurements in p -GaSe.

The attribution of the line E to a transition from a deep donor level to the valence-band continuum is consistent with its weak temperature dependence, at least up to 200 K. The sharp quenching above this temperature could be explained by the predominance at these temperatures of free-excitonic transitions. The lines F and G have a ΔE of 51 and 153 meV, respectively; the same considerations made for R_1 and R_2 can be applied to them.

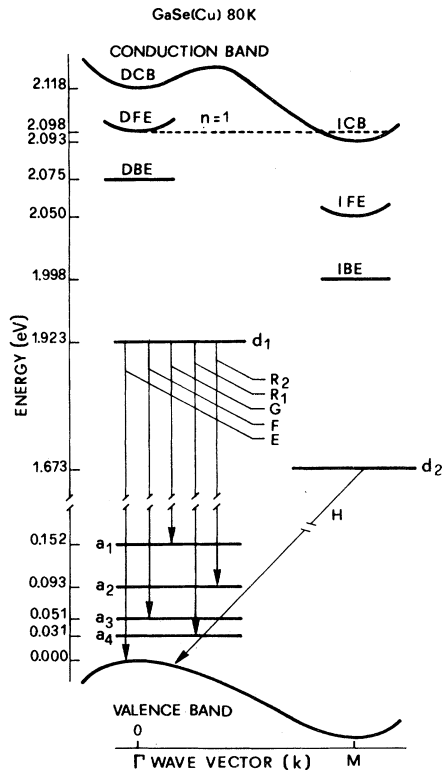


FIG. 6. Energy-level diagram of GaSe(Cu) at 80 K. The energies are measured from the top of the valence band (VB) toward the conduction band (CB). The extrinsic recombinations are indicated. DCB is the direct conduction-band minimum, DFE is the direct free-exciton level, and DBE is the direct bound-exciton level. d_1 and d_2 are donor levels and a_1 – a_4 are acceptor levels. The other symbols have the same meaning as those reported in Fig. 5.

As far as the excitation-intensity dependence of extrinsic bands is concerned, they are all sublinear or at most linear, as it is to be expected for transitions involving impurity levels. The most prominent features is the change of their exponent from $\gamma=0.5$ to $\gamma=1$ for E and F lines (see Table I), going from undoped to doped crystals. This fact can be qualitatively explained in a manner similar to that used for C and D lines, for which the competition with impurity transitions raises the exponent. In this case, this role could be played by R transitions, which start from the same level d_1 as the transition E and F do, i.e.,

TABLE II. Acceptor level energies deduced from the present work and comparison with those published by other authors.

Acceptor Levels	Present work (meV)	Comparison with acceptor levels of other authors (Refs.) (meV)	
a_1	152	150	28
a_2	93	86	27
		100	19
a_3	51	50	27
a_4	31	30	19

transitions R_1 and R_2 , which are absent in undoped samples.

The resulting level scheme of GaSe(Cu) is drawn in Fig. 6. In this figure, all the energy levels discussed above are reported, but only the extrinsic transitions are indicated. In Table II, the acceptor levels of GaSe(Cu) deduced by the present luminescence measurements are compared with those reported in the literature.

It is worth commenting briefly on the transitions between donor d_2 and acceptors a_1 – a_4 levels which are indeed possible in the scheme of Fig. 6. In fact, the luminescence of the line H , which is explained by a bound-free transition, is very weak (Figs. 1 and 2) and the transitions connecting the same donor level d_2 to localized states a_1 – a_4 are expected to have emission intensity comparable to that of the H band or smaller. These recombinations, if they exist, are in the infrared part of the spectrum and it should be very difficult to detect them, because the experimental apparatus loses sensitivity above 8000 Å.

V. CONCLUSIONS

The photoluminescence measurements carried out in GaSe and GaSe(Cu) in the photon energy range from 1.5 to 2.1 eV show the same lines in the intrinsic part of the spectrum, including direct and indirect excitonic emissions. On the other hand, the PL spectra of the two types of samples are different concerning radiative transitions in the forbidden energy gap, where donor-acceptor levels are involved. The comparison of spectra in undoped and Cu-doped crystals shows that two of the acceptor levels (a_2 and a_4 of Fig. 6) are directly connected to the Cu doping; the other energy levels including the donor states d_1 and d_2 could be linked to the defects which are present in GaSe crystals and which are enhanced by the doping. Moreover, the indirect channel recombination is strongly influenced by the density of the impurity levels present in the crystals.

The analysis of the spectra as a function of temperature and excitation intensity permits one to obtain a possible scheme of the donor-acceptor levels located in the forbidden energy gap of GaSe and involved in the radiative recombination observed in this work. The recombination model introduced explains the different temperature dependence found for the intrinsic lines: linear for the direct and indirect free-excitonic emissions; exponential for the direct and indirect bound-excitonic lines. Furthermore, this model also accounts for the excitation-intensity dependence of the luminescence of the free- and bound-excitonic emissions. This dependence is connected to the density of the impurity levels in the crystals. In fact, the linear behavior of these two last lines found in undoped samples becomes quadratic in doped crystals.

ACKNOWLEDGMENTS

The author is grateful to F. Lévy for providing some of the GaSe single crystals used in the experiment and to A. Minafra for stimulating and helpful discussions.

- ¹F. Hulliger, *Structural Chemistry of Layer-Type Phases*, edited by F. Lévy (Reidel, Dordrecht, 1976), Chap. IV, 5b.
- ²G. Ottaviani, C. Canali, F. Nava, P. Schmid, E. Mooser, R. Minder, and I. Zschokke, *Solid State Commun.* **14**, 933 (1974).
- ³V. Augelli, C. Manfredotti, R. Murri, A. Rizzo, and L. Vasaneli, *Nuovo Cimento* **47B**, 101 (1978).
- ⁴S. Nagel, A. Baldereschi, and K. Maschke, *J. Phys. C* **12**, 1625 (1979).
- ⁵M. Schlüter, *Nuovo Cimento* **13B**, 313 (1973).
- ⁶M. Schlüter, J. Camassel, S. Kohn, J. P. Voitchovsky, Y. R. Shen, and M. L. Cohen, *Phys. Rev. B* **13**, 3534 (1976).
- ⁷Y. Depeursinge, thesis No. 297, Ecole Polytechnique Fédérale, Lausanne, Switzerland, 1978 (unpublished).
- ⁸Le Chin Thanh and C. Depeursinge, *Solid State Commun.* **21**, 317 (1977).
- ⁹G. B. Abdullaev, G. L. Belenkii, E. Y. Salaev, and R. A. Suleimanov, *Nuovo Cimento* **38B**, 469 (1977).
- ¹⁰A. Mercier, E. Mooser, and J. P. Voitchovsky, *Phys. Rev. B* **12**, 4307 (1975).
- ¹¹E. Mooser and M. Schlüter, *Nuovo Cimento* **18B**, 164 (1973).
- ¹²E. Aulich, J. L. Brebner, and E. Mooser, *Phys. Status Solidi* **31**, 129 (1969).
- ¹³N. Kuroda and Y. Nishina, *Phys. Status Solidi B* **72**, 81 (1975).
- ¹⁴A. Mercier, E. Mooser, and J. P. Voitchovsky, *J. Lumin.* **7**, 241 (1973).
- ¹⁵A. Cingolani, F. Evangelisti, A. Minafra, and A. Rizzo, *Phys. Status Solidi A* **17**, 541 (1973).
- ¹⁶J. L. Staehli and A. Frova, *Physica* **99B**, 299 (1980).
- ¹⁷J. P. Voitchovsky and A. Mercier, *Nuovo Cimento* **22B**, 273 (1974).
- ¹⁸V. Capozzi, A. Cingolani, G. Mariotto, A. Minafra, and M. Montagna, *Phys. Status Solidi A* **40**, 93 (1977).
- ¹⁹Ph. Schmid, J. P. Voitchovsky, and A. Mercier, *Phys. Status Solidi A* **21**, 443 (1974).
- ²⁰G. Gobbi, J. L. Staehli, M. Guzzi, and V. Capozzi, *Helv. Phys. Acta* **52**, 9 (1979).
- ²¹E. Mooser (private communication).
- ²²V. Capozzi, *Phys. Rev. B* **23**, 836 (1981).
- ²³V. Capozzi and A. Minafra, *Solid State Commun.* **38**, 341 (1981).
- ²⁴T. Kushida, F. Minami, Y. Oka, Y. Nakazaki, and Y. Tanaka, *Nuovo Cimento* **39B**, 650 (1977).
- ²⁵D. G. Thomas, J. J. Hopfield, and W. M. Augustyniak, *Phys. Rev.* **140**, A202 (1965).
- ²⁶D. G. Thomas, M. Gershenzon, and F. A. Trumbore, *Phys. Rev.* **133**, A269 (1964).
- ²⁷C. Manfredotti, A. Rizzo, C. De Blasi, S. Galassini, and L. Ruggiero, *J. Appl. Phys.* **46**, 4531 (1975).
- ²⁸G. Fisher and J. L. Brebner, *J. Phys. Chem. Solids* **23**, 1369 (1962).